Porous-Resin-Supported Calcium Sulfate Materials for Thermal Energy Storage

Hongyu Huang,[a, b] Jun Li,*[c] Huhetaoli,*[a, b] Yugo Osaka,[d] Chenguang Wang,[a, b] Noriyuki Kobayashi,[c] Zhaohong He,[a, b] and Lisheng Deng[a, b]

A new porous-resin-supported calcium sulfate ($CaSO_4$-PSM) material with high-density and high reactivity for chemical heat storage is developed and characterized. The newly developed $CaSO_4$-PSM exhibits a higher reactivity than normal $CaSO_4$. Furthermore, the particle diameter is an important factor for the development of new chemical thermal energy storage (CTES) material. $CaSO_4$-PSM exhibits good performance in the hydration and dehydration processes when used as a CTES material. The hydration reaction rate of the particle with a diameter of 75 μm is 13.3 times of that of 750 μm, whereas, the dehydration reaction velocity is approximately 1.5 times higher. This finding is due to more abundant favorable pore channels for vapor transport and a larger specific surface area. Aggregation of the $CaSO_4$ particles before and after repetitive operations can be eliminated, and a good durability of the new porous supported thermal energy storage material of $CaSO_4$ can be obtained.

Introduction

Thermal energy storage has become one of the most important research topics in recent years, because of it enables reduced dependence on fossil fuels, mitigates greenhouse gas (CO_2) emissions, and enhances energy utilization efficiency.[1–4] Sensible thermal energy storage, latent thermal energy storage, and chemical thermal energy storage (CTES) are the three main types of thermal energy storage.[5,6] CTES is attracting considerable attention because of advantages including a broad range of working temperatures, a high energy storage density, and minimal loss of heat to the environment during storage.[7–10] However, to render the CTES technique available and efficient, suitable materials with appropriate reversible chemical reactions should be identified. Numerous CTES reaction systems, including hydride-,[11,12] hydroxide-,[13–15] redox-,[16,17] carbonate-,[18–21] and ammonium-based systems,[22–24] have been investigated for use in high operation temperature ranges of 573 K to 1273 K.

Oxide/hydroxide systems, such as magnesium oxide (MgO)[14] and calcium oxide (CaO),[13,15] are applied for heat pumps, heat storage, motor preheating, and similar applications. Kato et al.[14] developed an MgO/H_2O reaction heat pump system at a hydration temperature of 363 K to 443 K and a pressure of 31.2 kPa to 70.1 kPa. Hydration temperature and pressure vary with different CTES materials, which are the most important factors for the reactivity and durability of $MgO/Mg(OH)_2$ reaction heat pump system during repetitive reaction. A cycling study of the $MgO/Mg(OH)_2$ reaction system was reported by Ervin,[15] who showed that the dehydration and hydration conversion is initially 95%, declines to 60~70% within 40 cycles, and then remained stable for a subsequent 460 cycles. This result was mainly related to the volume changes of the heat storage material, which originated from agglomeration of the MgO particles during repeated cycling.

$CaO/Ca(OH)_2$ can be used as a typical CTES material, offering advantages of low material cost and high storage capacity at high temperature. Schaube et al.[25] investigated the application of the $CaO/Ca(OH)_2$ reaction system for CTES to improve the energy efficiency of power plants and recovery of process heat. They confirmed the cycling stability and identified the particle reaction rate as the main limiting factor in the test system. Ervin[15] first suggested the use of the $CaO/Ca(OH)_2$ reaction system in thermal energy storage and investigated the reactivity and durability of this system, reaching 211 cycles. Furthermore, the average reaction capacity of the $CaO/Ca(OH)_2$ reaction system was 95% and re-

[a] Prof. Dr. H. Huang, Dr. Huhetaoli, Prof. Dr. C. Wang, Dr. Z. He, L. Deng
Guangzhou Institute of Energy Conversion
Chinese Academy of Sciences
Guangzhou 510640 (PR China)
E-mail: taoli@ms.giec.ac.cn

[b] Prof. Dr. H. Huang, Dr. Huhetaoli, Prof. Dr. C. Wang, Dr. Z. He, L. Deng
Guangdong Key Laboratory of New and
Renewable Energy Research and Development
Guangzhou 510640 (PR China)

[c] Dr. J. Li, Prof. Dr. N. Kobayashi
Department of Chemical Engineering
Nagoya University
Nagoya, Aichi 464-8603 (Japan)
E-mail: junli@energy.gr.jp

[d] Dr. Y. Osaka
College of Science and Engineering
Kanazawa University
Kanazawa, Ishikawa 920-1192 (Japan)

Supporting Information and the ORCID identification number(s) for the author(s) of this article can be found under http://dx.doi.org/10.1002/ente.201600174.

mained constant throughout the 211 cycles. However, the reaction rate gradually decreased and stabilized at about 190 cycles. Schmidt et al.[26] experimentally investigated a 10 kW high-temperature thermochemical storage reactor based on CaO. They found that the dehydration and rehydration temperature were approximately 723 K and 823 K, respectively, with a reversible conversion of 77 % of the material and without degradation effects observed after 10 cycles. Conversion is evidently lower than that found during a previous thermogravimetric analysis (TGA)[25] because of material carbonization during handling. Watanabe et al.[27] produced a porous solid-supported $Ca(OH)_2$ chemical heat storage material with high reactivity and high durability. Its production process is shown in Figure 1.[27] The synthesized porous

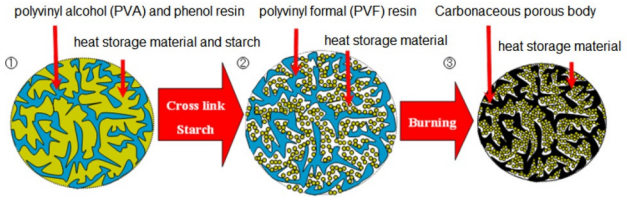

Figure 1. Production schematic diagram of porous carbon supported CTES material.

carbon-supported CTES material can be used as a high-performance material in CTES. A polyvinyl form resin-supported chemical heat storage material was treated by burning to form the carbon-supported chemical heat storage material of $Ca(OH)_2$, which can maintain high-performance after 15 CTES cycles.

Several CTES materials, such as $CaSO_4$, are available at low temperature, around and below 373 K, as from the reaction equilibrium lines of the hydration of $CaSO_4{\cdot}0.5\,H_2O$. The $CaSO_4$ and $CaSO_4{\cdot}0.5\,H_2O$ reaction system can be expressed by reaction (1):

$$CaSO_4(s) + 0.5H_2O\ (g) = CaSO_4 \cdot 0.5H_2O\ (s) + 16.8\ kJ\ mol^{-1} \quad (1)$$

The equilibrium pressure and temperature (P_{eq} and T_{eq}) of the $CaSO_4/CaSO_4{\cdot}0.5H_2O$ reaction system have been reported by Lee et al.[28] The equilibrium pressure and equilibrium temperature can be defined as the pressure and temperature at which the Gibbs free energy changes for the reaction equal zero ($\Delta G^0 = 0$).[29] At the equilibrium state, neither the forward nor the reverse reaction is favored. Lee et al.[28] experimentally investigated and calculated the equilibrium pressure of $CaSO_4/CaSO_4{\cdot}0.5\,H_2O$ reaction system with temperature. The reaction system showed a good agreement with theoretical calculation results using Ball and Norwood's equilibrium kinetics model.[30] The equilibrium pressure of the $CaSO_4/CaSO_4{\cdot}0.5\,H_2O$ reaction system can be expressed as $P_{eq} = 2.32 \times 10^7 exp(-65.3 \times 10^3/R_g T)$[28].

The $CaSO_4/CaSO_4{\cdot}0.5H_2O$ reaction system can store heat at approximately 423 K and release heat between 333 K and

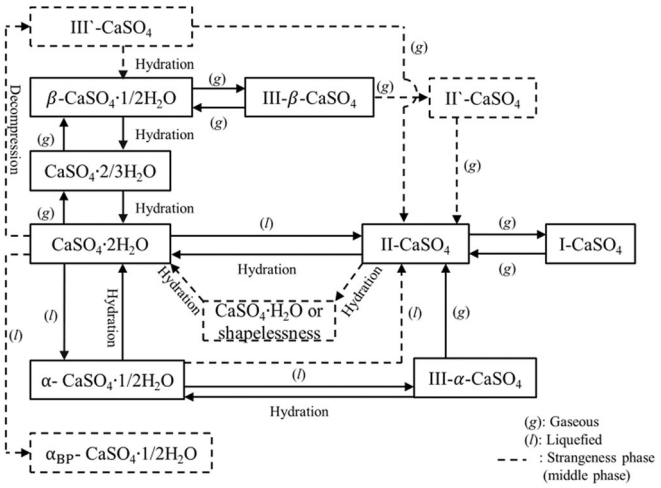

Figure 2. Various forms of $CaSO_4$ crystal structure and their interaction reaction.

373 K.[31] The conversion of the $CaSO_4/CaSO_4{\cdot}0.5H_2O$ reaction system usually decreases because of particle agglomeration and secondary interaction reactions of the CTES material. Several crystal structures of $CaSO_4$ play a role in the reaction system: $CaSO_4{\cdot}2\,H_2O$, $CaSO_4{\cdot}0.5\,H_2O$ (α or β types), III-$CaSO_4$ (α or β types), II-$CaSO_4$, and I-$CaSO_4$. Each hydrate can be formed by controlling the dehydration temperature. The secondary interaction reactions of these hydrates occur as shown in Figure 2. III-β-$CaSO_4$ can be transformed to II-$CaSO_4$ at around 673 K to 873 K, while $CaSO_4{\cdot}2\,H_2O$ can be transformed to II-$CaSO_4$ at around 363 K to 474 K.[31–33] Those secondary interaction reactions decrease the hydration/dehydration rate of CTES materials. The $CaSO_4{\cdot}0.5\,H_2O$ and $CaSO_4$ reaction pair can be applied in, for example, buildings or supercomputer centers that have low-temperature-level exhaust heat and high power demands for heating and cooling, with the following advantages:[27–29,34,35] (a) it is a safe reaction system, without pollution; (b) the reaction material can be easily obtained, at a low price; (c) the $CaSO_4$ reaction system is relatively easy to use because it does not attract moisture.

Hence, it is worthwhile to investigate the $CaSO_4{\cdot}0.5H_2O$/$CaSO_4$ reaction pair to provide fundamental data and knowledge for possible practical applications of this reaction system. However, because particle agglomeration, changes of crystal form, and secondary interaction reactions of $CaSO_4$ cause deterioration of CTES materials during repeated cycling, and limit its utilization in practical applications, eliminating these occurrences is the focus of this research.

Herein, we propose a new porous resin support method for $CaSO_4$ production to improve its properties as a CTES material and its CTES performance at low temperature. A method for the production of a material that enables thermal storage on a porous resin is proposed in this research. Porous support materials (PSMs) make up a new porous resin-supported thermal storage material. This research aims to produce and evaluate the energy storage performance of

$CaSO_4$-PSM at temperatures around and below 373 K. The specific objectives of this research are as follows: First, $CaSO_4$-PSM is produced using the porous resin-supported method. Scanning electron microscopy (SEM) and energy-dispersive X-ray (EDX) spectroscopy are employed to measure the surface properties of $CaSO_4$-PSM. Second, the hydration/dehydration characteristics of $CaSO_4$-PSM with different particle diameters are investigated through thermogravimetric analysis (TGA). Finally, the long-term morphological stability and maintenance of reactivity of the $CaSO_4$-PSM cycle hydration/dehydration reaction at a closed heat storage system is experimentally investigated.

Results and Discussion

Preparation of $CaSO_4$–PSM

We prepared the porous-resin-supported $CaSO_4$ in a five-step procedure. (1) The raw materials, shown in Table 1, were mixed for 10 min by using a mixer (25AM-QR, Shinagawa Machinery Works, Co., Ltd). (2) Cylindrical pellets were extruded by an twin-screw type pelletizer extruder (Figure 3, EXD-60, Dalton Co., Ltd). (3) The pellets from

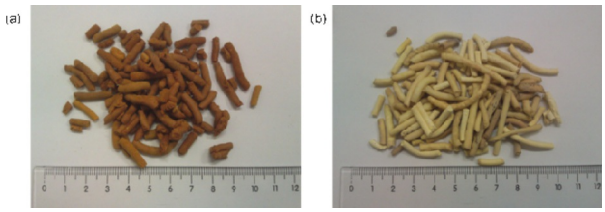

Figure 3. Base materials of porous material (without $CaSO_4$) (a) and porous resin supported CTES material (b).

step (2) were dried under a N_2 atmosphere for 8 h, yielding $CaSO_4$–PSM. (4) The porous-resin-supported materials from step (3) were stored under vacuum at 473 K for 30 min to remove residual volatiles. (5) Finally, $CaSO_4$–PSM was pulverized and sieved to obtain different $CaSO_4$–PSM particle diameters (75, 162, 375, and 750 μm). Scanning electron microscopy (SEM) and energy dispersive X-ray (EDX) images of $CaSO_4$–PSM before and after the hydration/dehydration reactions were obtained by using a JEOL Ltd. JSM-5600 V and an JEOL Ltd. JEM-2010 instrument, respectively.

To confirm the weight ratios of the supported $CaSO_4$, material 1 (without $CaSO_4$ as CTES material) and material 2 (resin-supported $CaSO_4$ material) were heated in a crucible by using a methane burner. The masses of material 1 and 2 were measured by a high-accuracy weight balance. The results are summarized in Table 2. The data for material 1 reveal that the polymer can be completely decomposed when heated for 2 h. Furthermore, only $CaSO_4$ is left for material 2 after 4 h of heat treatment because the polymer is completely decomposed. Therefore, the maximum weight ratio of $CaSO_4$ in the $CaSO_4$–PSM in this work is 55.6 %.

Table 2. Weight changes of materials 1 and 2 with time.

Sample	t [h] 0	2	4	Weight ratio of $CaSO_4$ [%]
material 1	0.1188	−0.0008	–	0.0
material 2	0.0927	0.0521	0.0515	55.6

TGA measurements

Thermogravimetric analysis (TGA) was performed by using a Shimatsu Co. TGA-50 instrument to measure the hydration/dehydration rates of $CaSO_4$–PSM based on the weight and temperature of materials during hydration and dehydration process (Figure 4). 10 mg of $CaSO_4$–PSM with a particle diameter in the range of 75 μm to 750 μm was used, with N_2 as carrier gas at a flow rate of 100 mL min^{-1}. Prior to the hydration/dehydration reaction, the temperature was increased to 393 K at 5 K min^{-1}. In the hydration reaction, the TGA temperature was lowered to 373 K at −5 K min^{-1}. The vapor pressure was set to 0.04 atm, and the hydration reaction began when TGA reached the target hydration temperature. The vapor pressure was set to 0.12 atm when the hydration reaction was completed, and then the TGA temperature was increased to 393 K at 2 K min^{-1}. The vapor was quenched, and the dehydration reaction began when the TGA temperature reached the target (393 K). Weight and temperature changes were measured during the hydration/dehydration reactions. The hydration/dehydration rates were calculated from the weight changes of reaction materials. The hydration rate and dehydration rate are expressed in Equations (1) and (2):

$$X_h = \frac{1 - W/W_0}{1 - M_{CaSO_4 \cdot 0.5H_2O}/M_{CaSO_4}} \quad (1)$$

Table 1. Raw material compositions of porous-resin-supported CTES materials.

Sample	S890[a] [g]	CTES material [g]	PVA 20[b] % [g]	35 % HNO_3 [g]	formaldehyde [g]	distilled water [g]
1[c]	120	phenolic resin	35	–	–	40
2[d]	120	200	70	4	6	70

[a] Granular phenolic resin (Air Water Inc.). [b] Poly(vinyl alcohol) resin (20 % aqueous solution, Kuraray Co., Ltd). 1[c] Base materials without CTES material of $CaSO_4$. [d] Porous resin-supported CTES material.

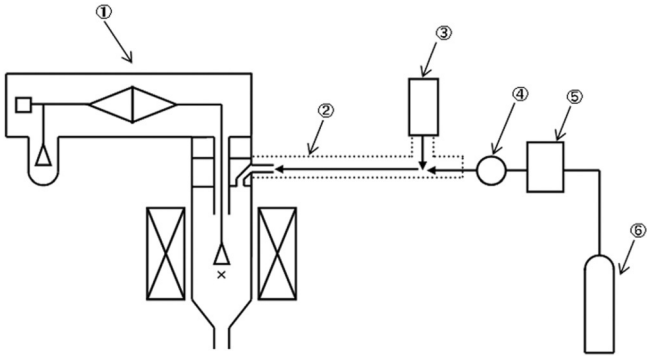

Figure 4. Schematic diagram of TGA system with vapor injection. Note: ① TGA-50; ② Ribbon heater; ③ Syringe pump of vapor; ④ Pressure gauge; ⑤ Flowmeter; ⑥ N_2.

$$X_d = \frac{1 - W/W_0}{1 - M_{CaSO_4}/M_{CaSO_4 \cdot 0.5H_2O}} \quad (2)$$

where X_h and X_d are the hydration rate and dehydration rate (−), W_0 is the weight of raw material (mg; excluding the polymer's weight), W is the weight of hydrated $CaSO_4$, and $M_{CaSO_4 \cdot 0.5H_2O}$ and M_{CaSO_4} are the mole weights of $CaSO_4 \cdot 0.5H_2O$ and $CaSO_4$ ($g\,mol^{-1}$). The subscripts h, d, and 0 refer to hydration, dehydration, and initial value, respectively.

Measurement at a closed system

A practical system was used to evaluate the reactivity performance of $CaSO_4$–PSM during the heat storage and release process. The apparatus used to evaluate the real heat storage and release process, as well as the durability of $CaSO_4$–PSM, is shown schematically in Figure 5. A stainless reaction tube (with inner diameter and height of 52 and 500 mm, respectively) was connected to an evaporator/condenser. The temperature of the reaction tube was controlled by a ceramic electric tube furnace (Sansyo Co., Ltd., ARF-80KC). In the heat storage process, the temperature of the reaction tube was set to 393 K, and the heat storage reaction time was 135 min. Subsequently, the temperature of the reaction tube was decreased to 333 K, and the evaporator temperature was set at 333 K. Heat release reaction time was 30 min. The heat storage and release process was repeated 40 times to evaluate the durability of $CaSO_4$–PSM.

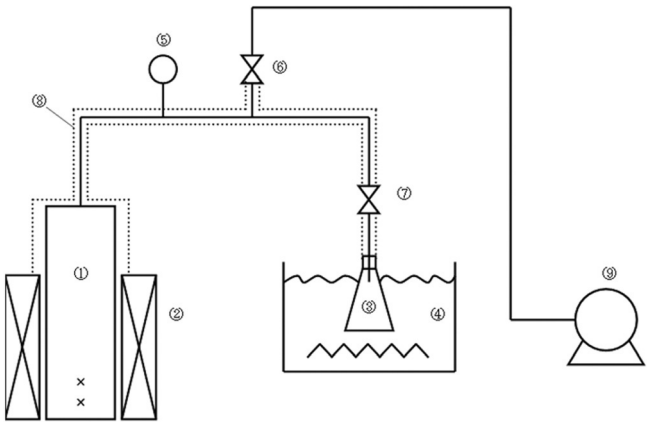

Figure 5. Schematic diagram of practical heat storage and release system. Note: ① Reactor; ② Electric tube furnace; ③ Evaporator/condenser; ④ Thermostatic bath; ⑤ Pressure gauge Flowmeter; ⑥ Value for vacuum pump; ⑦ Value for evaporator/condenser; ⑧ Ribbon heater; ⑨ Vacuum pump.

Characterization

SEM and EDX results are shown in Figures 6 and 7. The chemical compositions of $CaSO_4$–PSM, based on EDX, are shown in Table 3. $CaSO_4$ is supported well on the resin body, as shown in Figure 7. Furthermore, the distributions of C, Ca, O, and S are shown in Figure 6. In this image area, the weight ratio of Ca/S is 2.91 as shown in Table 2, which is higher than the ratio for stoichiometric $CaSO_4$, mainly because of a lower number of S atoms in this area, and higher in other image area (i.e., there is not an exact one-to-one ratio of Ca and S in this image area). The results confirm

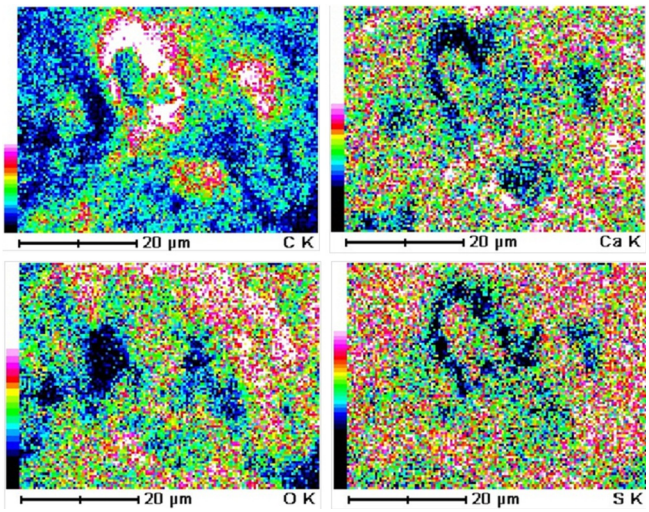

Figure 6. EDX (×5000 times) image of $CaSO_4$-PSM sample at particle diameter of 75 μm: element of C, Ca, O and S.

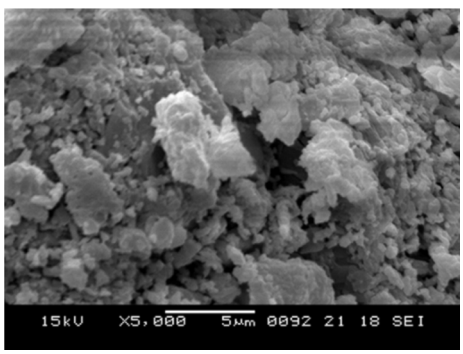

Figure 7. SEM (×5000 times) image of $CaSO_4$-PSM sample at particle diameter of 75 μm.

Table 3. C, O, S, and Ca compositions of $CaSO_4$-PSM from EDX.

Chemical element	Energy resolution [keV]	Weight composition [%]
C	0.277	34.92 ± 0.35
O	0.525	37.71 ± 1.14
S	2.307	7.00 ± 0.42
Ca	3.690	20.37 ± 0.85
Total	–	100.00

that the PSM thermal storage material can be successfully produced by the new porous resin-supported method.

Hydration and dehydration rate

Hydration and dehydration reaction rates were measured by TGA as shown in Figure 4. The effects of $CaSO_4$-PSM particle diameter on weight ratio of W/W_0 and the hydration rate of $CaSO_4$-PSM at 373 K are shown in Figure 8(a) and 8(b). The raw data of weight changes of $CaSO_4$-PSM based on hydrated $CaSO_4$ during the hydration reaction are summarized in the Supporting Information, Figure S1. Figure 8 shows that the weight ratio W/W_0 during the hydration of $CaSO_4$-PSM and $CaSO_4$ increases first and then remains constant with hydration time, which leads to the same trend of hydration rate with time. The hydration rate of $CaSO_4$-PSM was higher than that of normal $CaSO_4$. This finding is mainly attributed to the $CaSO_4$ particles that are well-supported in the pores of $CaSO_4$-PSM, as shown in the EDX image of $CaSO_4$-PSM

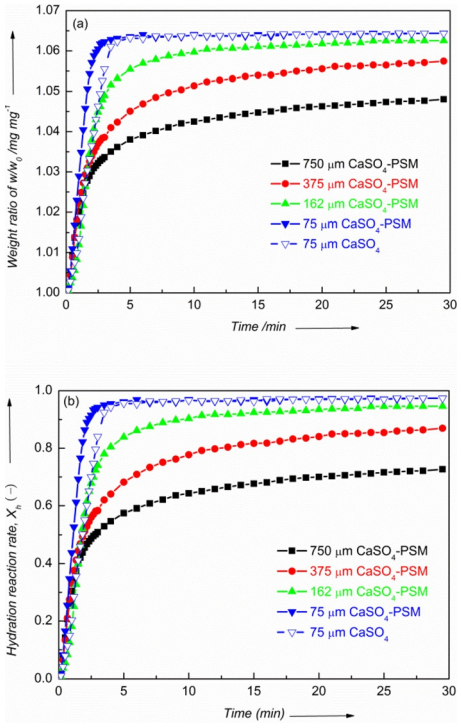

Figure 8. Effect of particle diameter on weight ratio of W/W_0 (a) and the hydration reaction rates of $CaSO_4$-PSM and $CaSO_4$ (b) at 373 K.

(Figure 6), which led to a higher hydration rate of $CaSO_4$-PSM. Furthermore, the hydration reaction rate decreases with increasing particle diameter. The hydration time at a hydration reaction ratio of 0.7 is 20.0 min when the particle diameter is 750 μm ($t_{750\text{-}hy}$ = 20 min), which is approximately 13.3 times that of particles with a diameter of 75 μm ($t_{75\text{-}hy}$ = 1.5 min). This is mainly due to the favorable pore channels for vapor transport in the $CaSO_4$-PSM particle. These channels can be observed from the pore distribution of $CaSO_4$-PSM (Figure 9), which was measured by mercury porosimetry (IV 9500, Shimadzu Co., Ltd). The cumulative and differential pore distributions of the $CaSO_4$-PSM sample are shown in Figure 9a and 9b. The diameter of the major pores in the $CaSO_4$-PSM sample were approximately 0.3 μm, and the total pore volume was 0.320 cm^3 g^{-1}. The pore channels are beneficial for vapor transport during the hydration/dehydration of $CaSO_4$-PSM when using $CaSO_4$-PSM as a new CTES material.

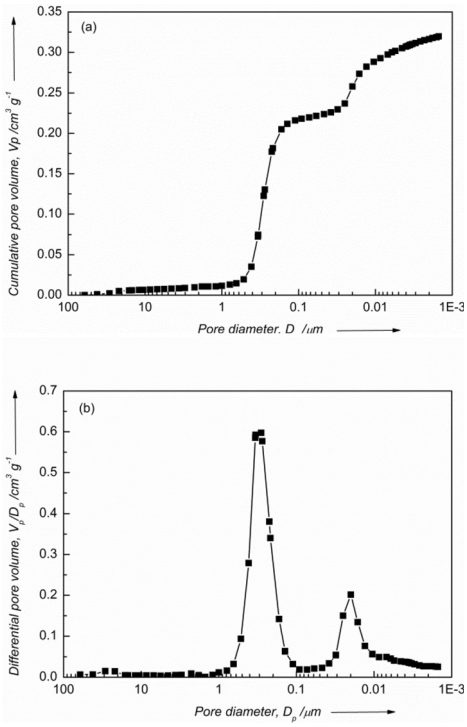

Figure 9. Pore distribution of $CaSO_4$-PSM sample at particle diameter of 75 μm: (a) cumulative pore distribution; (b) differential pore distribution.

Figure 10(a) and 10(b) show the effects of particle diameter of $CaSO_4$-PSM on weight rate of W/W_0 and the dehydration ratio of $CaSO_4$-PSM. Raw data on the weight changes of $CaSO_4$-PSM based on dehydrated $CaSO_4$ during dehydration are summarized in Supporting Information, Figure S2. The weight ratio of W/W_0 during the dehydration of $CaSO_4$-PSM and $CaSO_4$ increases firstly and finally keeps constant with dehydration time, causing a similar trend of dehydration rate with time. Furthermore, it shows that the dehydration reaction rate increased with decreasing particle diameter. Specifi-

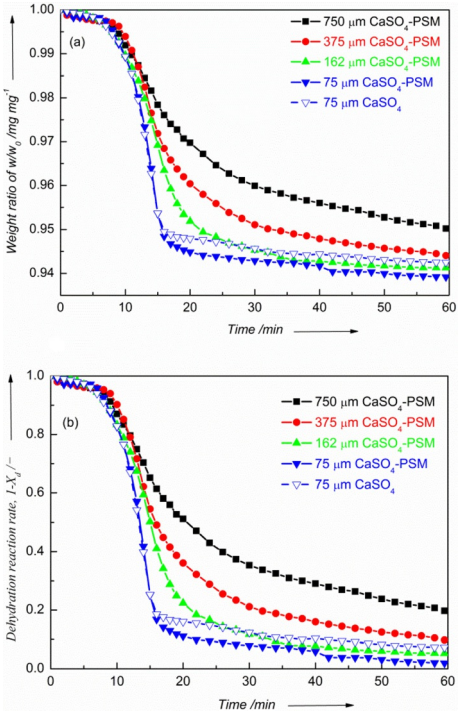

Figure 10. Effect of the particle diameter on weight ratio of W/W_0 (a) and the dehydration reaction rates of $CaSO_4$-PSM and $CaSO_4$ (b) at 393 K.

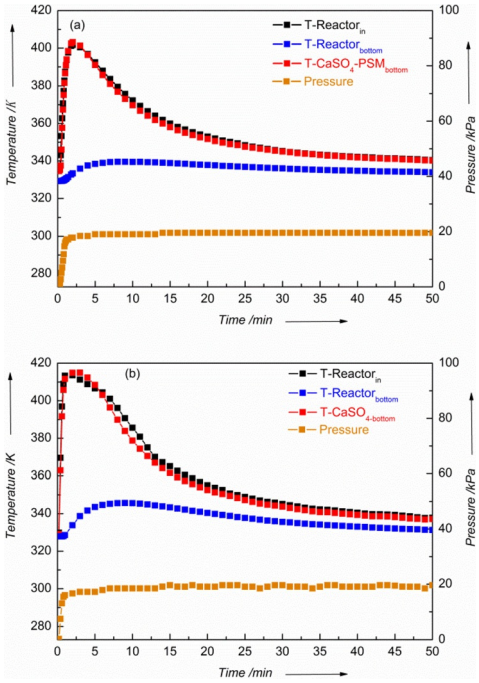

Figure 11. Temperature and pressure changes during heat storage process of $CaSO_4$-PSM (a) and $CaSO_4$ (b).

cally, the dehydration time at the dehydration reaction ratio of 0.7 was 37.0 min with a particle diameter of 750 μm ($t_{750\text{-}de}$ = 37.0 min), which is approximately 2.5 times of that with a particle diameter of 75 μm ($t_{75\text{-}de}$ = 14.7 min). Given these results, particle diameter is an important factor in using $CaSO_4$-PSM as a new CTES material. $CaSO_4$-PSM can be used as a new CTES material with good performance in the hydration/dehydration process. The reactivity and durability performance of $CaSO_4$-PSM as a new CTES material in practical systems are discussed in the following section.

Heat storage and release: Real process in a closed system

The system shown in Figure 5 was employed to evaluate the reactivity of $CaSO_4$-PSM during the heat storage and release process. In order to clarify the resistance during hydration/dehydration reactions, temperature changes during heat storage and release in the practical system were measured. The particle diameter of $CaSO_4$ and $CaSO_4$-PSM was 75 μm, which showed the best hydration and dehydration performance earlier. The mass fraction of $CaSO_4$ in $CaSO_4$-PSM is approximately 55.6 wt%. The temperature and pressure changes of $CaSO_4$-PSM and $CaSO_4$ during heat storage and release process are shown in Figure 11 and Figure 12. The black, red, and blue lines represent the temperature changes at the upper surface of heat storage materials in the reactor, at the bottom of heat storage materials along the centerline, and at the bottom of the reactor, respectively. The temperature differences between the surface and the middle of the heat storage materials (black line and red line in Figure 11a and Figure 12a) are small for $CaSO_4$-PSM, showing the

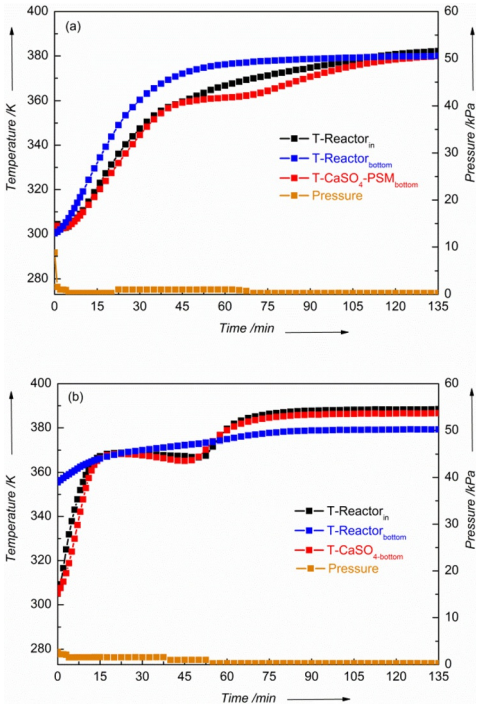

Figure 12. Temperature and pressure changes during heat release process of $CaSO_4$-PSM (a) and $CaSO_4$ (b).

better heat transfer ability of $CaSO_4$-PSM as compared to $CaSO_4$ (black line and red line in Figure 11b and Figure 12b). This indicates that $CaSO_4$-PSM possesses good heat transfer ability as a new CTES material in practical heat storage and release processes, despite the low ratio of $CaSO_4$ in $CaSO_4$-PSM 55.6 wt%.

Durability of $CaSO_4$–PSM

The heat release process can reduce the durability of $CaSO_4$-PSM. The effect of cycle number on repetitive durability of $CaSO_4$-PSM was experimentally measured. Repetitive operations of 40 cycles were measured for $CaSO_4$ and $CaSO_4$-PSM. Temperature changes with 10, 20, 30, and 40 cycles for $CaSO_4$ and $CaSO_4$-PSM during repetitive operations in the heat release process are shown in Figure 13a. The peak release temperature of both $CaSO_4$ and $CaSO_4$-PSM during the heat release process could be reached within 5 min. Thus, $CaSO_4$-PSM showed a rapid heat release rate when used as a new practical heat storage material.

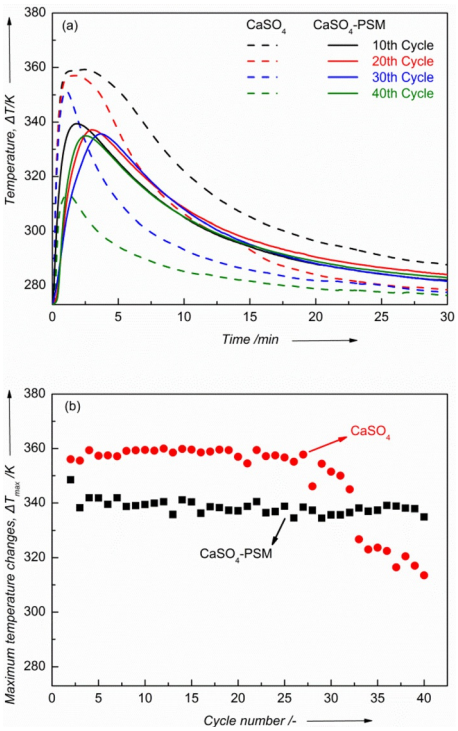

Figure 13. Temperature changes with time (a) and maximum temperature changes with cycle number (b) during heat release process of $CaSO_4$ and $CaSO_4$-PSM

A comparison of the maximum temperature of $CaSO_4$ and $CaSO_4$-PSM with cycle number is shown in Figure 13b. The maximum temperature changes of $CaSO_4$ decreased from approximately 30 cycles, which is mainly because of the aggregation of $CaSO_4$ particles before and after repetitive operations, as showed in the SEM images of the $CaSO_4$ sample before and after repetitive operations in Figure 14a and 14b. Although, the maximum temperature of $CaSO_4$-PSM is a little lower than that of $CaSO_4$, the maximum temperature of $CaSO_4$ decreases from 30 cycles and becomes lower than that of $CaSO_4$-PSM. Therefore, $CaSO_4$-PSM can maintain the same maximum temperature changes without any decrease, which can be confirmed by the comparison of the SEM images of $CaSO_4$-PSM before and after repetitive operation as shown in Figure 14c and 14d. Evident aggregation

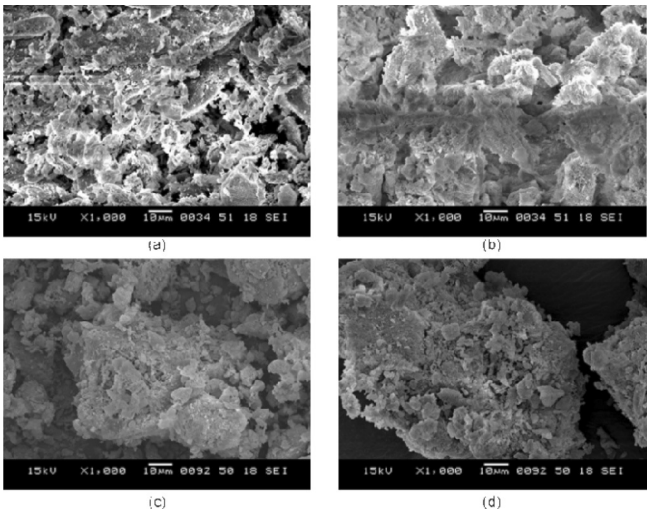

Figure 14. SEM images of samples (particle diameter: 75 μm): (a) $CaSO_4$ sample before repetitive experiment; (b) $CaSO_4$ sample after 40 recycle; (c) $CaSO_4$-PSM sample before repetitive experiment; (d) $CaSO_4$-PSM sample after 40 recycle.

of $CaSO_4$-PSM before and after repetitive operations was absent. Therefore, the new production method in this research for porous supported material proved to be an effective and favorable method for the development and production of new thermal heat storage materials around and below 373 K.

Conclusions

A porous-resin-supported material for chemical heat storage based on the hydration/dehydration cycle of $CaSO_4$ is developed. The porous-resin-supported $CaSO_4$ chemical heat storage material ($CaSO_4$–PSM) was extensively characterized. We found that:

(1) The $CaSO_4$ particles are successfully supported in the new $CaSO_4$–PSM material, which showed higher reactivity than unsupported $CaSO_4$;

(2) Particle diameter is an important factor when using $CaSO_4$–PSM as a new chemical thermal energy storage (CTES) material. The pores of the newly developed $CaSO_4$–PSM are beneficial for vapor transport and the material shows good performance in the hydration/dehydration process;

(3) Aggregation of $CaSO_4$–PSM particles before and after repeated operations can be eliminated, thus imparting good durability to the newly developed $CaSO_4$–PSM thermal energy storage material.

Acknowledgements

This study is supported by the National Natural Science Foundation of China (No. 51541609) and the Science and Technology Major Project of Guangdong (No.2013A011402006).

Keywords: calcium · energy storage · porous materials · sulfates · thermodynamics

[1] F. Agyenim, N. Hewitt, P. Eames, M. Smyth, *Renewable Sustainable Energy Rev.* **2010**, *14*, 615–628.
[2] K. E. N'Tsoukpoe, H. Liu, N. L. Pierrès, L. Luo, *Renewable Sustainable Energy Rev.* **2009**, *13*, 2385–2396.
[3] W. Wongsuwan, S. Kumar, P. Neveu, F. Meunier, *Appl. Therm. Eng.* **2001**, *21*, 1489–1519.
[4] P. Pardo, A. Deydier, Z. Anxionnaz-Minvielle, S. Rougé, M. Cabassud, P. Cognet, *Renewable Sustainable Energy Rev.* **2014**, *32*, 591–610.
[5] S. Hongois, F. Kuznik, P. Stevensc, J. Roux, *Sol. Energy Mater. Sol. Cells* **2011**, *95*, 1831–1837.
[6] N. Yu, R. Z. Wang, L. W. Wang, *Prog. Energy Combust. Sci.* **2013**, *39*, 489–514.
[7] D. S. Ovoshchnikov, I. S. Glaznev, Yu. I. Aristov, *Kinet. Catal.* **2011**, *52*, 620–628.
[8] B. Zajaczkowski, Z. Królicki, A. Jeżowski, *Appl. Therm. Eng.* **2010**, *30*, 1455–1460.
[9] C. Wang, L. Feng, H. Yang, G. Xin, W. Li, J. Zhang, W. Tian, X. Li, *Phys. Chem. Chem. Phys.* **2012**, *14*, 13233–13238.
[10] I. Glaznev, I. Ponomarenko, S. Kirik, Y. Aristov, *Int. J. Refrig.* **2011**, *34*, 1244–1250.
[11] B. Bogdanović, A. Ritter, B. Spliethoff, *Angew. Chem. Int. Ed. Engl.* **1990**, *29*, 223–234; *Angew. Chem.* **1990**, *102*, 239–250.
[12] M. Felderhoff, B. Bogdanović, *Int. J. Mol. Sci.* **2009**, *10*, 325–344.
[13] J. Obermeier, B. Müller, K. Müller, W. Arlt, *Energy Technol.* **2016**, *4*, 123–135.
[14] Y. Kato, J. Nakahata, Y. Yoshizawa, *J. Mater. Sci.* **1999**, *34*, 475–480.
[15] G. Ervin, *J. Solid State Chem.* **1977**, *22*, 51–61.
[16] M. A. Fahim, J. D. Ford, *Chem. Eng. J.* **1983**, *27*, 21–28.
[17] R. G. Bowrey, J. Jutsen, *Sol. Energy* **1978**, *21*, 523–525.
[18] A. Meier, E. Bonaldi, G. M. Cella, W. Lipinski, D. Wuillemin, R. Palumbo, *Energy* **2004**, *29*, 811–821.
[19] K. Kyaw, M. Kanamori, H. Matsuda, M. Hasatani, *J. Chem. Eng. Jpn.* **1996**, *29*, 112–118.
[20] R. Barker, *J. Appl. Chem.* **1974**, *24*, 221–227.
[21] R. Barker, *J. Appl. Chem.* **1973**, *23*, 733–742.
[22] K. Lovegrove, A. Luzzi, I. Soldiani, H. Kreetz, *Sol. Energy* **2004**, *76*, 331–337.
[23] K. Lovegrove, G. Burgess, J. Pye, *Sol. Energy* **2011**, *85*, 620–626.
[24] A. Luzzi, K. Lovegrove, E. Filippi, H. Fricker, M. Schmitz-geob, M. Chandapillai, S. Kaneff, *Sol. Energy* **1999**, *66*, 91–101.
[25] F. Schaube, A. Kohzer, J. Schütz, A. Wörner, H. Müller-Steinhagen, *Chem. Eng. Res. Des.* **2013**, *91*, 856–864.
[26] F. Schaube, A. Wörner, R. Tamme, *J. Sol. Energy Eng.* **2011**, *133*, 031006.
[27] F. Watanabe, S. Tsumagari, H. Huang, M. Hasatani, N. Kobayashi, O. Tsubouchi, N. Shiomi, *Kagaku Kogaku Ronbunshu* **2013**, *39*, 378–383 (Japanese).
[28] S. K. Lee, H. Matsuda, M. Hasatani, *Kagaku Kogaku Ronbunshu* **1986**, *12*, 75–82 (in Japanese).
[29] H. Zhang, K. Huys, J. Baeyens, J. Degrève, Y, Lv, *Energy Technol.* **2016**, *4*, 341–352.
[30] M. C. Ball, L. S. Norwood, *J. Chem. Soc. A* **1970**, 1476–1479.
[31] J. H. Lee, H. Ogura, S. Sato, *Appl. Therm. Eng.* **2014**, *63*, 192–199.
[32] J. H. Lee, Y. Otsubo, H. Ogura, *Proceedings of the 6th Asia Drying Conference*, Bangkok, Thailand **2009**, 232–236.
[33] Y. Arai, *Gypsum Lime* **1980**, *167*, 135–142.
[34] B. Zalba, J. M. Marín, L. F. Cabeza, H, Mehling, *Appl. Therm. Eng.* **2003**, *23*, 251–283.
[35] H. Zhang, J. Baeyens, G. Cáceres, J. Degrève, Y, Lv, *Prog. Energy Combust. Sci.* **2016**, *53*, 1–40.

Received: March 12, 2016
Revised: May 16, 2016
Published online on August 24, 2016

